# Mitigation of Earthquake-Induced Catastrophic Landslide Hazard on Gentle Slopes by Surface Loading

Aurelian C. Trandafir,[1)] Roy C. Sidle[2)] and Toshitaka Kamai[2)]
*1) Department of Geology & Geophysics, University of Utah, 135 South 1460 East Rm 717, Salt Lake City, Utah 84112-0111, USA. E-mail addresses: atrandafir@yahoo.com, a.trandafir@utah.edu.*
*2) Slope Conservation Section, Geohazards Division, Disaster Prevention Research Institute, Kyoto University, Gokasho, Uji, 611-0011, Kyoto, Japan.*

## Abstract

The present study evaluates a procedure based on applying an additional confining stress on the surface to increase the stability of gentle slopes along relatively shallow sliding surfaces in liquefiable soils subject to catastrophic failure during earthquakes. The surface pressure can be developed by thin bearing plates placed on the slope face and tied back with prestressed steel anchors which penetrate through the soil mass well beyond the potential sliding surface. The investigation is based on a modified sliding block model to estimate the earthquake-induced undrained displacements, which incorporates the sensitivity of computed displacements to variations in yield acceleration. Results of a dynamic displacement analysis addressing the undrained seismic performance of a gentle infinite slope that experienced different levels of increase in effective confining stress due to a uniform load applied normal to the surface, illustrate the effectiveness of this measure in mitigating the earthquake-induced catastrophic landslide hazard.

**Keywords:** slopes, earthquakes, seismic displacements, soil pressure, landslide hazard mitigation

## Introduction

Catastrophic landslides have repeatedly occurred on gentle slopes (i.e., 10° to 20°) during past earthquakes in Japan, sometimes causing great loss of life and significant environmental damage. Several examples of such earthquake-induced catastrophic failures have been reported in the literature (e.g., Sassa 1996; Yoshida et al. 2001; Matsuo et al. 2002). Additionally, investigations of the spatial distribution and features of landslides triggered by the October 23, 2004, Chuetsu earthquake in Niigata Prefecture, Japan revealed that 23% of the landslides mapped within a 2.9 km radius around the major earthquake epicenter occurred on slopes with gradients between 10° and 20° (Sidle et al. 2005). Past experience demonstrated that earthquake-induced catastrophic landslides on gentle slopes occurred along shear surfaces in saturated cohesionless materials, and laboratory shear tests on soil specimens collected from the landslide site revealed a gradual loss in undrained shear resistance after failure throughout the progress of shear displacement (Sassa 1996). This liquefaction phenomenon culminated in undrained ultimate steady state strengths smaller than the static (gravitational) driving shear stress along the sliding surface of the investigated landslides. Thus, the experimental results demonstrated the susceptibility of the sliding mass to an accelerated motion under static conditions (i.e., catastrophic failure) if the shear strength loss due to some transient disturbance (e.g., earthquake) was sufficient to definitively bring the shear resistance along the sliding surface below the gravitational driving shear stress. The present study evaluates a procedure based on applying an additional confining stress on the surface by means of prestressed ground anchors to increase the seismic stability of gentle slopes along relatively shallow sliding surfaces in liquefiable soils susceptible to catastrophic failure (Fig. 1).

Anchor systems have been extensively used over the past 50 years to stabilize dangerous slopes to a specified safety factor provided their significant technical advantages associated with substantial cost savings and reduced construction period. Successful applications of this technique to slope stabilization have been reported in the literature (e.g., Tan et al. 1985; Hashimoto et al. 1986; Corona 1996). Typically, the stability of slopes reinforced with anchors is assessed by the conventional limit equilibrium approach which is based on the concept of safety factor, and the anchor effect is quantified by considering an additional line load acting either at the ground surface where the anchor head is located (e.g., Hryciw 1991; Yamakawa 1995) or at the intersection point between the potential sliding surface and the anchor axis (e.g., GEO-SLOPE International Ltd 1993).

Due to the sensitivity of undrained yield resistance to progressive shear deformation noted in the case of previously mentioned earthquake-induced catastrophic landslides, this study employs however a sliding

pp. 515–521 

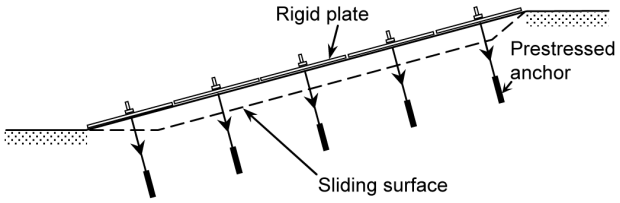


**Fig. 1.** Schematic of a tieback system for application of surface pressure.

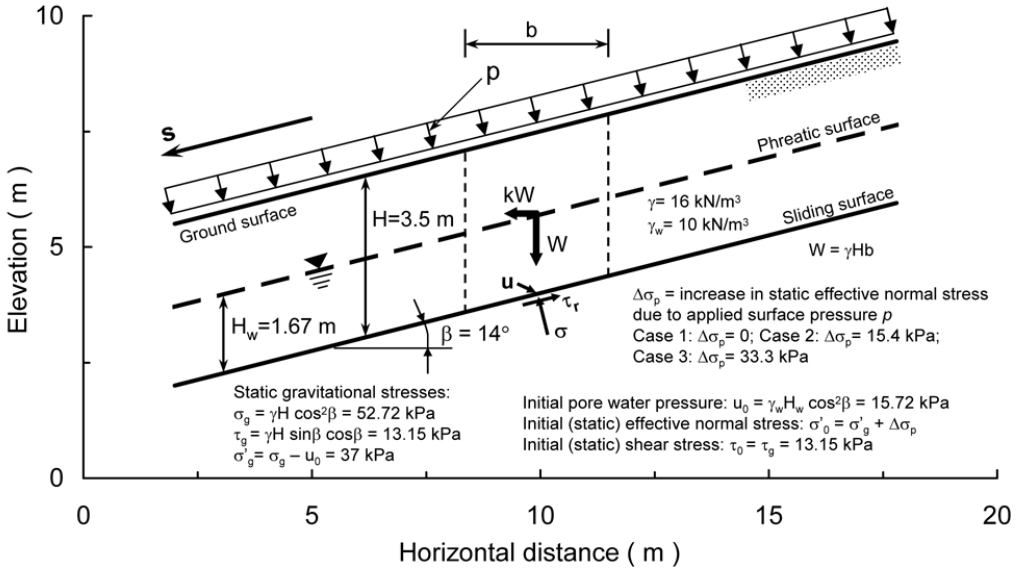


**Fig. 2.** Sample slope subjected to various intensities of applied surface pressure.

block approach (rather than a limit equilibrium analysis) to investigate the effectiveness of a surface pressure generated by thin bearing plates placed on the slope face and tied back with prestressed ground anchors in enhancing the stability of a gentle slope in liquefiable soil susceptible to a catastrophic failure during earthquake. The case analyzed in this paper corresponds to an infinite slope subjected to a uniformly distributed pressure, $p$, acting normal to the ground surface, as shown in Fig. 2. In these circumstances, only the static effective normal stress on the sliding surface ($\sigma_0'$) would increase due to the applied surface pressure $p$, while the static driving shear stress ($\tau_0$) would remain equal to the gravitational driving shear stress ($\tau_g$). The slope characteristics (Fig. 2) were selected based on the initial geometry of a catastrophic translational landslide, i.e., Tsukidate landslide, triggered by the 26-May-2003 Sanriku-Minami earthquake in Tsukidate town, Miyagi Prefecture, Japan (Trandafir and Sassa 2004a, 2005b). The soil properties above the sliding surface of the slope are those of the saturated silty sand found at the Tsukidate landslide site (Fig. 2). Three cases of surface pressure intensities associated with increments of static effective normal stress on the slip surface ($\Delta\sigma_p$) of 0 kPa (i.e., no surface loading), 15.4 kPa, and 33.3 kPa were analyzed (Fig. 2). For the assumed initial stress conditions, the undrained seismic slope performance was examined using a sliding block formulation developed by Trandafir and Sassa (2005a) to assess the earthquake-induced undrained displacements on shear surfaces in a saturated cohesionless soil for conditions of no shear stress reversals on the sliding surface, summarized in the following.

## Equation of motion and yield resistance-displacement curves

Assuming the slide mass in Fig. 2 is a rigid body in translation, driven downslope by a horizontal seismic force, the equation of motion may be written as

$$\ddot{s} = (a - k_y g)\cos\beta \tag{1}$$

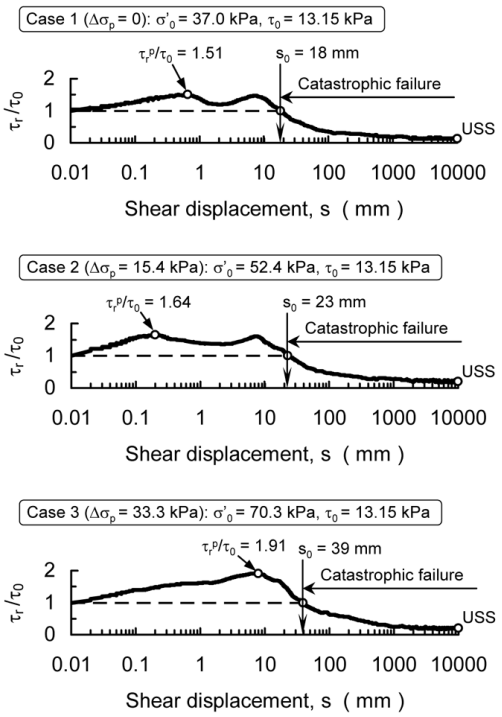


**Fig. 3.** Yield resistance -displacement curves for various increments of increase in effective normal stress on the sliding surface. USS, ultimate steady state.

where $\ddot{s}$ represents the relative acceleration in the direction parallel to the sliding surface, $\beta$ is the infinite slope angle, a is the horizontal earthquake acceleration, $g$ is gravitational acceleration, and $k_y$ is the yield coefficient. The horizontal earthquake acceleration coefficient, $k$, rendering the inertia force, $kW$, in a soil column of width $b$ and weight $W$ (Fig. 2), represents the ratio between the horizontal earthquake acceleration and gravitational acceleration (i.e., $k = a/g$). It is worth mentioning that $a$ and $\ddot{s}$ in Eq. (1) are functions of time, $t$ (i.e., $a = a(t), \ddot{s} = \ddot{s}(t)$).

The horizontal yield coefficient for undrained conditions on the sliding surface is given by the following equation:

$$k_y = (\tau_r/\tau_0 - 1)\tan\beta \tag{2}$$

where $\tau_r$ is the undrained yield resistance of the soil on the sliding surface.

Equation (2) makes use of the shear resistance-displacement relationship from undrained monotonic shear tests (Fig. 3) in order to update the value of the undrained yield coefficient of the sliding mass for a specific value of shear displacement during the earthquake. Therefore, a step-by-step numerical integration is required to calculate the dynamic displacements. In the numerical procedure, the excitation time is divided into a series of small increments, $\Delta t$, and by the linear acceleration method (Biggs 1964), the relative velocity, $\dot{s}(t + \Delta t)$, and the displacement of the slide mass, $s(t + \Delta t)$, at time $t + \Delta t$ can be calculated knowing the previous values, $\dot{s}(t)$ and $s(t)$, at time $t$:

$$\dot{s}(t + \Delta t) = \dot{s}(t) + \frac{\ddot{s}(t) + \ddot{s}(t + \Delta t)}{2}\Delta t \tag{3}$$

$$s(t + \Delta t) = s(t) + \dot{s}(t)\Delta t + \frac{2\ddot{s}(t) + \ddot{s}(t + \Delta t)}{6}\Delta t^2 \tag{4}$$

Notice that $\ddot{s}(t+\Delta t)$ in Eqs. (3) and (4) is a function of $k_y$ at $t+\Delta t$ according to Eq. (1). Since $k_y$ at $t+\Delta t$ depends on $\tau_r(t+\Delta t)/\tau_0$ which is a function of the unknown displacement $s(t+\Delta t)$ (Fig. 3), Eqs. (3) and (4) become nonlinear for the modified sliding block formulation used in this study. However, with reference to Fig. 3, the shear resistance-displacement curves considered in this paper do not show sharp variations in shape for very small increments of displacement. Therefore, in order to avoid numerical instabilities likely with an iterative process, for a sufficiently small time increment, $\Delta t$, a constant value of $k_y$ may be assumed within the current time interval, derived from $\tau_r(t)/\tau_0$ corresponding to $s(t)$ calculated from the previous integration step. Subsequently, the yield coefficient for the next integration step is updated based on $\tau_r(t+\Delta t)/\tau_0$ corresponding

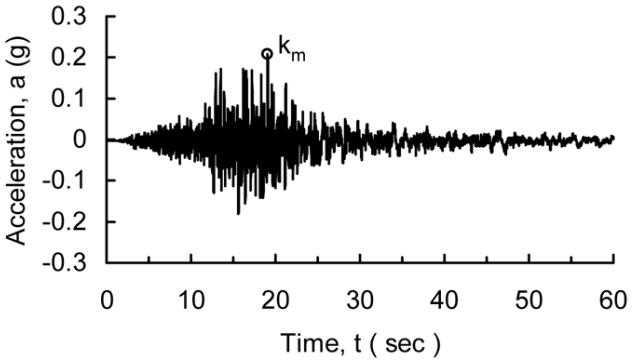


**Fig. 4.** Input horizontal earthquake record.

to the calculated displacement $s(t + \Delta t)$ at the end of the current time interval. For a time increment ($\Delta t$) of 0.001 sec which was used in the dynamic calculations, this approximation gave very accurate results. Results of undrained monotonic and cyclic ring shear tests on the silty sand considered in this analysis (Trandafir and Sassa 2004a, 2005c) and on clean sand (Trandafir and Sassa 2005a), as well as predictions of undrained cyclic shear response of saturated sand in a ring shear apparatus (Trandafir and Sassa 2004b) demonstrate the accuracy of using (in dynamic calculations) the shear resistance-displacement relationship from undrained monotonic shearing (Fig. 3) as an estimate of the undrained yield resistance under seismic conditions for no shear stress reversals on the sliding surface.

The yield resistance-displacement relationships used in this analysis (Fig. 3) were obtained from undrained monotonic ring shear tests (Trandafir and Sassa 2004a, 2005c) conducted for initial stress conditions associated with the cases analyzed in Fig. 2. Apparently, the data in Fig. 3 indicate ultimate steady state (USS) strengths after failure smaller than static driving shear stress, $\tau_0$. In these circumstances, a shear displacement at the end of seismic excitation exceeding the critical level $s_0$ is regarded as a "catastrophic failure" (Trandafir and Sassa 2005a) since the sliding mass is expected to develop an accelerated motion even after the earthquake loading has ceased, due to the static driving shear stress exceeding the undrained yield resistance on the slip surface (Fig. 3). The critical shear displacement ($s_0$) appears to increase with increasing initial effective normal stress on the sliding surface (Fig. 3). Also, the higher the initial effective normal stress, the higher the peak yield resistance ratio, $\tau_r^p/\tau_0$.

Trandafir and Sassa (2004a) investigated the influence of the vertical component of earthquake acceleration on the undrained seismic performance of the sample slope depicted in Fig. 2. According to the computational results, the accuracy of estimated undrained seismic displacements was not significantly affected by neglecting in dynamic calculations the vertical component of earthquake acceleration. Therefore, the simplification made in the present study by considering only the horizontal component of earthquake acceleration seems reasonable.

## Computational Results

The undrained seismic performance of the sliding mass shown in Fig. 2 was investigated for the input horizontal accelerogram depicted in Fig. 4. The acceleration data were recorded during the 26 May 2003 Sanriku-Minami earthquake at Mizusawa K-net station (station code IWT011) which has the same epicentral distance as the site of Tsukidate landslide triggered by this seismic event. The acceleration data in Fig. 4 correspond to the orientation of the investigated slope, as described by Trandafir and Sassa (2004a). Positive values on the accelerogram are associated in this analysis with horizontal inertia forces due to the earthquake driving the sliding mass downslope, thus corresponding to the direction of $kW$ in Fig. 2. For all of the numerical results presented herein, the condition of no shear stress reversals on the sliding surface (which is essential in the applicability of the previously introduced sliding block formulation) was satisfied during the calculated dynamic response.

Figure 5 shows the evolution of earthquake-induced undrained displacement, $s$, (relative to the critical displacement, $s_0$) for the cases of initial stress conditions on the sliding surface depicted in Fig. 3. It appears that with no surface loading (i.e., case 1 in Fig. 5), the deformation of the sliding mass reaches the critical stage (i.e., $s = s_0$) during strong ground motion, thus experiencing a catastrophic failure. For the other two cases, the sliding mass performed well under the input seismic excitation exhibiting limited permanent displacements smaller than $s_0$. The results indicate that increments of increase in static effective normal stress

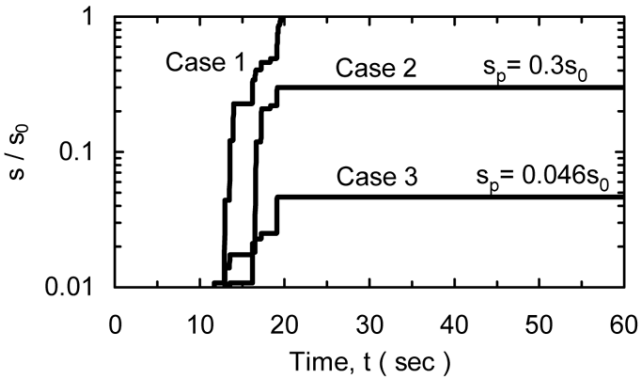


**Fig. 5.** 5 Evolution of undrained displacements during earthquake.

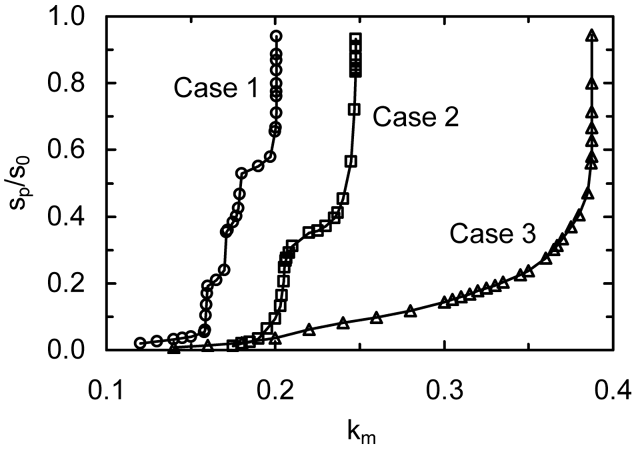


**Fig. 6.** Permanent displacement, $s_{\mathrm{p}}$, (relative to the critical displacement, $s_0$) versus coefficient of peak earthquake acceleration, km.

on the sliding surface ($\Delta\sigma_p$) representing 42% and 90% of the gravitational effective normal stress ($\sigma'_g$) reduce the earthquake-induced permanent displacements ($s_p$) to 30% and 5%, respectively, of the critical displacement ($s_0$).

The diagrams depicted in Fig. 6 were obtained by scaling the input seismic record to different values of the peak earthquake acceleration ($k_m$ in Fig. 4) and computing the corresponding earthquake-induced undrained permanent displacements. A non-linear relationship between the permanent displacement, $s_p$, and the peak earthquake acceleration coefficient, $k_m$, characterizes all three cases (Fig. 6). As noted by Trandafir and Sassa (2005a, b), this type of chart is useful in evaluating the catastrophic landslide hazards based on the magnitude of earthquake-induced permanent displacement. Apparently, the range of peak earthquake acceleration coefficients located on the quasi-linear portion of the ($s_p/s_0$)-$k_m$ curve (i.e., safe zone), becomes broader with increasing the static effective confining stress on the slip surface; thus, resulting in greater $k_m$ values necessary to attain the critical level of deformation $s_0$ (Fig. 6). The coefficient of critical peak earthquake acceleration, $k_{mc}$, defined by Trandafir and Sassa (2005a) as the peak earthquake acceleration associated with a permanent displacement $sp = s_0$ (or the minimum peak earthquake acceleration to trigger a catastrophic failure), is given in Fig. 7 in relation to the increment of static effective normal stress on the sliding surface. According to these data, $k_{mc}$ increased by 23% and 93% due to an increase in static effective normal stress by 42% and 90%, respectively.

## Conclusions

A numerical study was undertaken to investigate the effects of increasing the static effective confining stress on the stability of a gentle slope in liquefiable soil susceptible to catastrophic failure during earthquakes. By increasing both the yield acceleration and the magnitude of critical shear displacement, this possible mit-

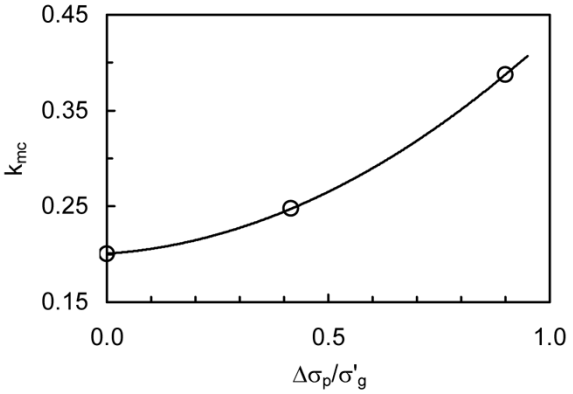


**Fig. 7.** Coefficient of critical peak earthquake acceleration, $k_{mc}$, in relation to the increment of increase in static effective normal stress, $\Delta_p$.

igation measure involving ground anchors prestressed against thin bearing panels placed on slope face, may reduce the earthquake-induced permanent displacements and, in the same time, may increase the threshold of peak earthquake accelerations that could trigger a catastrophic landslide.

## Acknowledgement

The first author gratefully acknowledges the Japan Society for the Promotion of Science (JSPS) Post-doctoral Research Fellowship.

## References

Biggs, J.M. (1964) Introduction to Structural Dynamics. McGraw-Hill Book Co., Inc., New York, NY, 341 pp.

Corona E.P. (1996) Stabilization of excavated slopes in basalt. *Proc., 7th Int. Symp. on Landslides*, Trondheim, Norway, 16–21 June 1996, Vol. 3, 1771–1776, Balkema, Rotterdam, The Netherlands.

GEO-SLOPE International Ltd. (1993) Computer program *SLOPE/W* for slope stability analysis. User's guide, Version 2, Calgary, Alberta, Canada.

Hashimoto I, Kawasaki K. and Kodera H. (1986) Cases of landslide control by dead-anchors. *Proc., 21st Japan National Conference on Soil Mechanics and Foundation Engineering*, Sapporo, 1483–1486 (in Japanese).

Hryciw R.D. (1991) Anchor design for slope stabilization by surface loading. *Journal of Geotechnical Engineering ASCE* **117**(8),1260–1274.

Matsuo, O., Saito, Y., Sasaki, T., Kondoh, K. and Sato, T. (2002) Earthquake-induced flow slides of fills and infinite slopes. *Soils and Foundations* **42**(1), 89–104.

Sassa, K. (1996) Prediction of earthquake induced landslides. *Proc., 7th Int. Symp. on Landslides*, Trondheim, Norway, 16–21 June 1996, Vol. 1, 115–132, Balkema, Rotterdam, The Netherlands.

Sidle, R.C., Kamai, T. and Trandafir, A.C. (2005) Evaluating landslide damage during the 2004 Chuetsu earthquake, Niigata, Japan. *Eos, Transactions, American Geophysical Union* **86**(13), 133, 136.

Tan, S.B., Tan S.L., Yang K.S. and Chin Y.K. (1985) Soil improvement methods in Singapore. *The 3rd International Geotechnical Seminar*, Nanyang Technological Institute, Singapore, 249–272.

Trandafir, A.C. and Sassa, K. (2004a) Newmark deformation analysis of earthquake-induced catastrophic landslides in liquefiable soils. *Proc., 9th Int. Symp. on Landslides*, Rio de Janeiro, 28 June–2 July 2004, Vol. 1, 723–728, Balkema, Rotterdam, The Netherlands.

Trandafir, A.C. and Sassa, K. (2004b) Undrained cyclic shear response evaluation of sand based on undrained monotonic ring shear tests. *Soil Dynamics and Earthquake Engineering* **24**, 781–787.

Trandafir, A.C. and Sassa, K. (2005a) Seismic triggering of catastrophic failures on shear surfaces in saturated cohesionless soils. *Canadian Geotechnical Journal* **42**(1), 229–251.

Trandafir, A.C. and Sassa, K. (2005b) Evaluation of catastrophic landslide hazard on gentle slopes in liquefiable soils during earthquakes. *Proc., Int. Conf. on Landslide Risk Management*, Vancouver, Canada, 31 May–3 June 2005, 629–635, Balkema, Rotterdam, The Netherlands.

Trandafir, A.C. and Sassa, K. (2005c) Earthquake-induced catastrophic landslide risk evaluation in liquefiable soils. *Annuals of Disaster Prevention Research Institute, Kyoto University*, **48C**, 143–151.

Yamakawa O. (1995) Simplified design method of slope reinforced with piles and anchors. Ph.D. Thesis, The University of Tokushima, (in Japanese).

Yoshida, N., Nishi, M. and Nanbu M. (2001) Damage to residential fills in the 1995 Hanshin-Awaji earthquake. *Natural Hazards* **23**, 87–97.